NASA/TM-20220011775

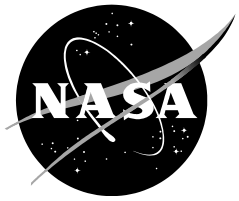

Mission Radiation Environment Modeling and Analysis

Avionics Trade Study for GCD Rad-Neuro Project

Richard L. Alena
NASA Ames Research Center

August 2022

NASA STI Program ... in Profile

Since its founding, NASA has been dedicated to the advancement of aeronautics and space science. The NASA scientific and technical information (STI) program plays a key part in helping NASA maintain this important role.

The NASA STI program operates under the auspices of the Agency Chief Information Officer. It collects, organizes, provides for archiving, and disseminates NASA's STI. The NASA STI program provides access to the NTRS Registered and its public interface, the NASA Technical Reports Server, thus providing one of the largest collections of aeronautical and space science STI in the world. Results are published in both non-NASA channels and by NASA in the NASA STI Report Series, which includes the following report types:

- TECHNICAL PUBLICATION. Reports of completed research or a major significant phase of research that present the results of NASA Programs and include extensive data or theoretical analysis. Includes compilations of significant scientific and technical data and information deemed to be of continuing reference value. NASA counterpart of peer-reviewed formal professional papers but has less stringent limitations on manuscript length and extent of graphic presentations.

- TECHNICAL MEMORANDUM. Scientific and technical findings that are preliminary or of specialized interest, e.g., quick release reports, working papers, and bibliographies that contain minimal annotation. Does not contain extensive analysis.

- CONTRACTOR REPORT. Scientific and technical findings by NASA-sponsored contractors and grantees.

- CONFERENCE PUBLICATION. Collected papers from scientific and technical conferences, symposia, seminars, or other meetings sponsored or co-sponsored by NASA.

- SPECIAL PUBLICATION. Scientific, technical, or historical information from NASA programs, projects, and missions, often concerned with subjects having substantial public interest.

- TECHNICAL TRANSLATION. English-language translations of foreign scientific and technical material pertinent to NASA's mission.

Specialized services also include organizing and publishing research results, distributing specialized research announcements and feeds, providing information desk and personal search support, and enabling data exchange services.

For more information about the NASA STI program, see the following:

- Access the NASA STI program home page at http://www.sti.nasa.gov

- E-mail your question to help@sti.nasa.gov

- Phone the NASA STI Information Desk at 757-864-9658

- Write to:
  NASA STI Information Desk
  Mail Stop 148
  NASA Langley Research Center
  Hampton, VA 23681-2199

NASA/ TM-20220011775

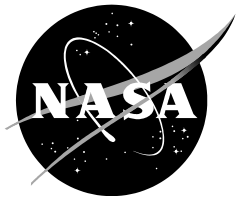

Mission Radiation Environment Modeling and Analysis

Avionics Trade Study for GCD Rad-Neuro Project

Richard L. Alena
NASA Ames Research Center

National Aeronautics and
Space Administration

NASA Ames Research Center, Moffett
Field, CA 94035

August 2022

Acknowledgments

The author wishes to acknowledge the contributions of the NASA Electronic Parts Program (NEPP) for providing significant information regarding radiation test and device characteristics. Also acknowledged are the NASA Ames RadNeuro team for providing the support needed to complete this analysis and the Code R TechEdSat Team for supporting the flight demonstration.

Table of Contents

List of Figures and Tables

Introduction

The two main objectives of this trade study are characterizing the mission radiation environment for multiple Design Reference Missions (DRM) and analysis of radiation effects on avionics with the goal of producing radiation tolerant Neuromorphic Computing processor chips with innovative radiation-induced fault mitigation. The NASA process for defining radiation requirements for flight avionics is applied to this domain.[i] The effects of trapped protons and electrons in the Van Allen radiation belts predominates in Low-Earth-Orbit (LEO) and the solar wind, solar flares and Galactic Cosmic Rays (GCRs) are the dominant radiation challenge in the open space between the planets of our solar system. The nature and energy of the particles that cause circuit upset and failure is very different in the two regimes. Two results are produced from the radiation models: determining the Total Integrated Dose (TID) experienced by avionics for a given DRM and predicting the Single Event Effects (SEE) rates for avionics during high rate exposure. These tools are applied to existing semiconductors and can be used for predicting the radiation performance of future semiconductors based on early radiation testing of new devices.

Modeling Tools and Methods

The project ran its own simulations using the Space Environment Simulator (SPENVIS) hosted by ESA and containing the definitive radiation models for Earth orbit, lunar orbit and Mars and Jupiter orbits.[ii] These radiation models are verified from spacecraft data so produce good correlation with actual mission environments. The process begins by defining trajectories and orbits for the DRMs used in the trade study.

Several underlying radiation models are used for the numerical simulation tools that produce results characterizing the specific DRM radiation environment and the effects on semiconductors. The radiation models correspond to the natural phenomenon producing ionizing radiation. Starting from the Earth's surface, the first major radiation source encountered in LEO are the Van-Allen trapped radiation belts, which are produced by the solar wind's interaction with the magnetosphere. A proton belt is situated under the electron belt and both are modeled using the AP-8 and AE-8 tools. The belts and the parameters used in the models are shown in the figure below.[iii]

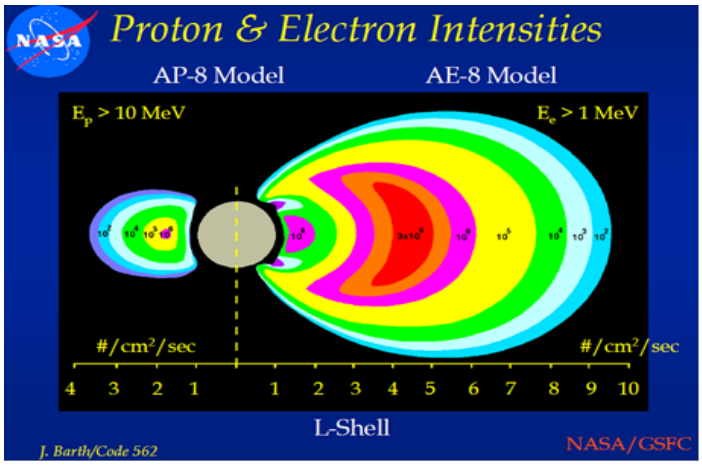

Figure 1 Van Allen Radiation Belts and AE-8/AP-8 Model Values

As one leaves the protective environment of the magnetosphere, the contribution from solar flares greatly increases while the trapped radiation contribution goes to zero. In a similar fashion, GCRs also increase as one leaves the magnetosphere's shielding.

Solar emission models are used for characterizing the statistical nature of solar flares or solar particle events (SPE). The ESP model is used to define the energies and flux coming from the Sun.[iv] The figure below helps to understand the nature of solar flares. While major events occur about four times a year, minor events are occurring much more frequently, and contribute to total dose and SEE rates. Solar Protons are the major species, but Helium and heavier ions are also present and are called Solar Ions. Generally, particle flux is expressed in number of particles per second per unit area. Solar Flares are expressed in fluence, (particles/sec-m2-steradian) which is flux per unit angle when the radiation source is isotropic. Fluence is also time-integrated flux, where the period is generally a year. These events can contribute significantly to avionics failures so this model is very important beyond GEO. Please note that the solar sunspot cycle modulates the activity level of SPEs. This means that the start date and duration of a mission with respect to the solar cycle is a key variable.

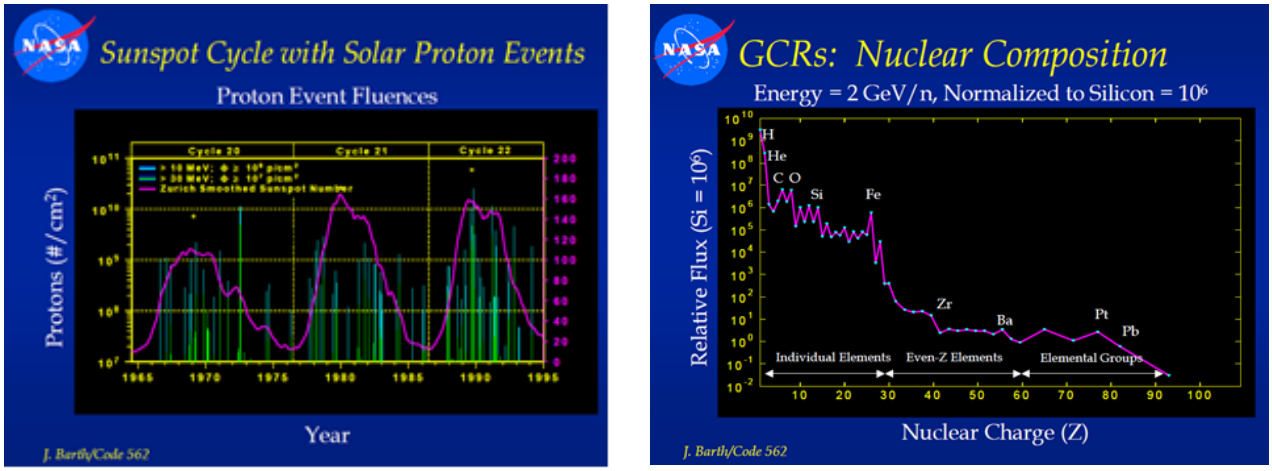

Figure 2 Solar Proton Event Model and Galactic Cosmic Ray Composition

The PSYCHIC model is used for GCRs, which originate outside the solar system and which are considered isotropic in nature. Despite the name, GCRs are predominantly alpha particles, or He nuclei traveling at high-speed and therefore capable of inducing significant energy into irradiated material. Heavier ions, up to Iron, are also present, and can cause multiple upsets due to their high energy. Ions heavier than iron are produced by supernovae. GCR dose contributions and SEE rates are included in the radiation analysis tools. The graph below represents the underlying radiation model used for GCRs.[v]

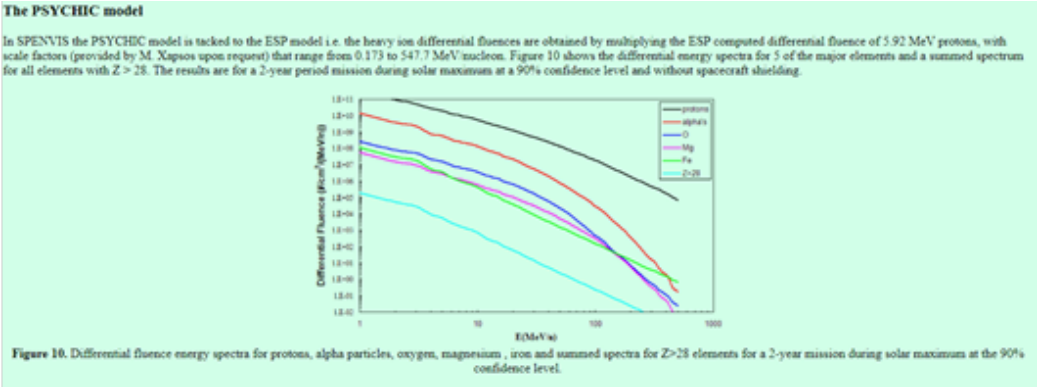

Figure 3 PSYCHIC GCR Model

Generally, the radiation environment is characterized by flux vs energy graphs, which will be presented in detail in a subsequent section. Separate graphs for trapped particles, SPEs and

GCRs are generated in their native coordinate systems. The key output of the radiation modeling are these numerical representations of the energy, number and species of the specific radiation. To determine relevant parameters such as Total Integrated Dose, maximum dose during SPE, average dose including SPE contributions, GCR contributions requires integrating the incident flux with the interaction cross-section of Silicon for each species and for each energy level. Since each input is a complex function, the use of numerical integration is required: linear assumptions and extrapolations are completely inaccurate; the integration must be performed in the native coordinate system of the model and the summation of the contributions must take into account the effect of shielding by aluminum or any other material comprising the avionics housing. The immediate results of these numerical simulations are a graph of Total Integrated Dose (TID) vs the thickness of Aluminum shielding from the spacecraft and avionics housing.

The SPENVIS workbench uses widely accepted codes that also can predict Single Event Effects (SEE) rates for a given semiconductor that has been characterized during testing for radiation susceptibility. Radiation testing using either protons or heavy ions produces a graph of the Linear Energy Threshold (LET) values vs energy for the chosen species. The LET graphs allow calculation of SEE rates by integrating over the incident radiation energy and flux expected for a given DRM. The key output from SPENVIS are not the graphs and reports, but rather the datasets that are used as input to the TID and SEE rate prediction tools like CREME96. The complexity of this analysis drove the need to standardize the radiation models and the computational tools to ensure accuracy and the ability to compare the results of different projects.

While there are many references to specific space radiation environments, certain radiation fields are highly localized and therefore, a given mission trajectory can experience a significant difference in radiation levels compared to similar ones. Therefore, full-up simulation of a proposed mission's radiation environment and the use of these simulation tools to predict the spacecraft's avionics SEE performance and its effective TID is critical.

Avionics Systems Radiation Engineering Process

Radiation induced damage and transient errors in avionics systems are characterized into broad categories:

- Single-Event Functional Failures (SEFI) or Single-Event Latchup (SEL) – failures caused by particle radiation-induced charge injection causing a chip to fail permanently or transiently until power is cycled.
- Single-Event Upset (SEU) – change in the value of a digital memory caused by a single particle changing the state of the memory circuit.
- Total Integrated Dose (TID) – change in semiconductor device performance due to accumulated particle dose over a wide range of energies and particle species.

Each type of failure is analyzed and mitigated differently and this trade study will define these distinctions. NASA has a defined process for avionics system engineering that has been tailored to radiation tolerance.[vi] The process can be outlined:

- Define Design Reference Missions (DRM) for the avionics
- Define the operating conditions for the avionics
- Model the radiation environment for the chosen DRM
- Define avionic system requirements w.r.t. radiation levels
- EEE Parts selection to meet requirements
- Inclusion of radiation mitigation circuits such as ECC and watchdog timers
- Avionics system verification

This trade study has defined numerous DRMs from benign LEO to GTO and Lunar/Mars missions requiring high levels of radiation tolerance. The trade study presents the radiation environment for the DRM, determines TID dose over the entire mission duration and can predict SEE rates once the LET of the semiconductor device is determined. The underlying code for TID is SHIELDOSE-2 and the underlying code for SEE rate is CREME96, both used extensively for this purpose. The goal is to execute an avionics system radiation hardening effort using new neuromorphic chips and to quantify the benefit of the multiple methods. The methods range from hardening the semiconductor devices themselves, adding shielding to reduce dose, adding circuits for monitoring and redundancy (i.e. watchdog timer and error correcting code for memory) and finally using dual or triple cross-checking processor architecture for covering errors.

Design Reference Mission Definition

The DRM definition started with three different LEO orbits: a benign one with little radiation, an orbit similar to the ISS at 51 degree inclination and a polar LEO orbit. Most missions have to traverse this region, so this is relevant to nearly any mission beyond LEO. In contrast, GEO is outside the trapped Van Allen radiation belts, so encounters more Galactic Cosmic Rays (GCR) and is less shielded from Solar Particle Events (SPE) such as solar flares or mass ejections. High radiation missions were chosen to represent deep space missions beyond LEO. The GTO is used to place satellites in GEO by successively raising the perigee and lowing the apogee until the design GEO orbit is attained. In this process, GTO produces very high radiation levels because it passes through the trapped radiation belts at least twice a day. Once circularized, the orbit has the lower radiation levels of GEO.

Additional DRMs were defined for lunar and Mars missions. The Earth's magnetosphere extends out to 65,000 Km, well beyond the 38,000 GEO orbit, providing some shielding from GCR and SPEs. However at a lunar orbit of 385K Km from Earth, there is no shielding from the magnetosphere, so this region is called open space and is the defined radiation environment for the cruise phase to other planets. The DRM also addresses the lunar and Mars orbit and surface cases.

LEO Orbits

The orbital cases were chosen to represent the most common ones used for actual missions. Only orbits around the Earth are analyzed, with Lunar orbits also defined as geocentric. Certain flux graphs are presented for all the DRM cases below. For LEO orbits, trapped electrons and protons in the Van Allen radiation belts are the primary radiation source and occur in distinct belts around the Earth as shaped by the solar wind's interaction with the magnetosphere.

LEO Zero: 500 Km, zero inclination orbit

This orbit was chosen to represent the minimum radiation case, where the Earth's magnetosphere fully shields the spacecraft from ionizing radiation. The spacecraft trajectory misses the South Atlantic Anomaly (SAA) and never gets near the polar regions. The Trapped Particles are at their minimum for LEO, producing at most only 10 Rads of total dose for an entire year. Proton and electron fluxes are measured in particles per second per square centimeter and can go up to a few hundred particles per second at maximum. There is zero solar flare content - the magnetospheres' shielding is that effective. The GCR contribution is also very low, a factor of five below a more inclined orbit.

LEO ISS: 500 Km, 51 degrees inclination

This orbit was chosen to represent the average orbit of the ISS. It goes through the SAA multiple times a day (9/15 orbits) and gets near the polar regions with their enhanced particle

flux. The trapped particles, protons and electrons, are now showing a big flux difference due to the anisotropic nature of proton and electron radiation belts around the Earth. This orbit crosses both of them. The proton flux is 10 times higher than the LEO Zero case, but the electron flux is higher by a factor of one thousand. Total dose is now 200 Rads per year, mostly from the trapped particles of the Van Allen belts. Solar flare contributions are now comparable to trapped radiation numbers, but still very low, particularly given the short duration and low periodicity. GCR contributions are five times that of LEO Zero, but still far below the values seen outside the magnetosphere.

LEO Polar: 500 Km 89 degree inclination

This orbit represents common polar orbits used for reconnaissance and earth observation. It is highly similar to the LEO-ISS case with the orbit taking the spacecraft through the SAA and near the poles. There is more electron activity for this orbit vs the ISS one as these species are more abundant at the poles.

LEO Orbit Summary

LEO orbits are dominated by the shielding of the Earth's magnetosphere, which greatly lowers the contribution from solar particle events. It also greatly lowers the GCR rate as well. The trapped particles are higher in energy than the solar wind due to the magnetosphere acting as a cyclotron, raising the energy of the incident radiation by trapping and concentrating them. This moves the proton energy to where it can cause issues with avionics. For LEO, we present the simulation data for only the trapped particles, although the tables include all contributions. Trapped particles are assumed to be directional, so flux is given as number of particles per second per unit area (cm^2) and the target is assumed to be planar. Trapped protons in LEO orbit range in flux from 30 particles/sec-cm^2 in the benign regions to over 200,000 when in the SAA or near the poles. Electrons are more prevalent near the poles and range from 10,000 to 1,000,000, both in the SAA and near the poles. The energy ranges from 0.1 Mev to around 50 MeV for protons, which are in the range that produces effects in semiconductors.
The proton trapped particle flux are shown in terms of their energy and against orbital time in the graphs taken from the LEO-ISS case. Two distinct features are noted:

- Proton flux decreases exponentially from 0.1 MeV to nearly 100 MeV
- The proton flux vs orbital time shows big peaks of 10E5/sec-cm2 when traversing the SAA

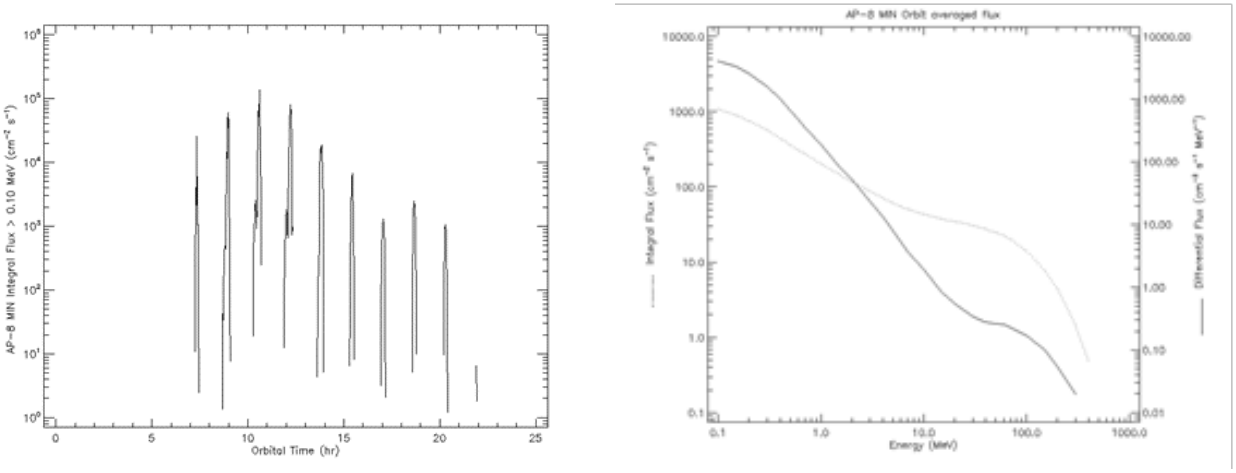

Figure 4 LEO-ISS Trapped Proton Flux vs Energy and Proton Flux vs Orbital Time Graphs

The calculation of TID is performed using SHIELDOSE-2, which integrates the contributions from all sources and species impacting on Silicon sitting in the middle of a hollow aluminum

shielding sphere of varying thickness. One must take into account the effects of shielding for this calculation, in that the contributions from low energy particles below 1 MeV are dominant, yet do not affect avionics since all avionics has some level of shielding due to packaging. Using this method, the TID from all sources, protons, electrons, Bremstralung and Solar Protons can be determined. Huge numbers of low energy particles are blocked by even simple shields and therefore do not contribute to either TID or SEE.

GEO Orbits

Geosynchronous orbits (GEO) are far away from the Earth so that the orbital period equals the rotational period, making a spacecraft appear to hover over a given location on the Earth's surface. All true GEO orbits are equatorial due to geometry. It is known that GEO orbits, which are used extensively for communication satellites, pose a high radiation challenge particularly during solar flares. At this distance, the spacecraft is beyond the influence of the magnetosphere-induced Van Allen radiation belts, but is still shielded to some extent. The day side of the magnetosphere is about 65K Km from Earth, so a GEO orbit is still within the influence of the magnetosphere and its shielding. However, the Van Allen radiation belts are below GEO orbits, so trapped particle effects are minimal.

GEO Orbit: 38K Km altitude, 0 degree inclination

A spacecraft in GEO orbit is often used for communications with a lifetime of around 10 years. Both the need for reliability and its long mission duration require radiation hardness and this analysis will quantify both flux and total dose.
For GEO, the trapped particles are non-existent, so flux is zero. In contrast, the solar flare fluence is 10,000,000 particles at 10 MeV dropping to 1,000,000 particles at 50 MeV. This fluence is a factor of three higher than a polar LEO orbit, showing the large increase in solar flare effects from even the worst-case LEO orbit. He nuclei due to solar flares vary from 10,000 to 100,000 particles, much higher than the polar LEO except for high energy He nuclei.
The GCR contribution is about 3000 particles/sec-m^2-steradian, which is a factor of six over LEO orbits. The TID goes up to 2K Rad per annum.

GTO Orbit" 38K X 500 Km altitude, 0 degree inclination

A Geosynchronous Transfer Orbit (GTO) is a method for boosting the orbit of a satellite to a higher GEO orbit by simultaneously raising the perigree while lowering the apogee, circularizing the orbit to the GEO altitude. During this phase, the spacecraft sees the trapped radiation belts twice each day as it dips into the magnetosphere and sees the open space environment for the rest of the time where solar flares and GCRs dominate. This orbit produces the highest TID of any of those analyzed due to this double dose.

For GTO, proton flux from trapped particles are similar to that of polar LEO orbits, but with a much reduced duty cycle. Trapped electrons are not present. The 50 MeV solar flare proton numbers are very similar to GEO, while the 10 MeV He nuclei are similar.
The GCR contribution is about 3000 particles/sec-m2-steradian, which is a factor of six over LEO orbits. The TID goes up to 100K Rad per annum, by far the worst dose of any of the orbits.

Lunar and Mars Mission Radiation Environments

Beyond GEO is considered open space where the primary radiation sources are Solar protons, Solar Particle Events (SPE: solar flares and Coronal Mass Ejections (CME)) and GCRs. These trajectories take the spacecraft beyond the shielding effects of the Earth's atmosphere and magnetosphere. The SPEs and GCRs are isotropic, coming into a given device from all directions and are expressed in spherical coordinates.

GEO is typically defined as 38K Km altitude and zero inclination and marks a certain transition zone between LEO and open space. The magnetosphere's shielding extends to 65K Km, so GEO is still partially shielded from solar protons and ions, SPEs and GCRs, but now well beyond any trapped radiation belts. Therefore the trapped proton and electron contributions go down, while the contributions from solar protons/ions, SPEs and GCRs go up and reach their maximum value well before one reaches the Moon.

Cruise Phase Radiation Environment

The SPENVIS radiation modeling and analysis tool can be used for calculating the radiation environment for a cruise to the Moon. The magnetosphere is actually a teardrop, shaped by the solar wind. SPENVIS incorporates a high-fidelity magnetosphere model that includes effects in these transition zones. By the time the spacecraft has reached the average Moon distance of 385K Km from Earth, there is virtual no atmospheric nor magnetospheric shielding of either SPE or GCRs, so this regime is typical of cruise environments for Lunar and Mars missions.
The method chosen to explore the Lunar (and Mars) cruise phase is to run a SPENVIS simulation using a geocentric altitude of 385 K Km, the average distance between the Earth and Moon. It should be noted that the limit of this geocentric altitude is 1M Km in SPENVIS. For verification, a simulation was run at this maximum altitude and results were the same as the Lunar orbit case.
The Lunar Orbit graphs and numbers show the expected phenomena:

- Contributions from the trapped proton and electron belts are ZERO (GEO still has radiation from this source)
- Solar SPE numbers expressed as solar protons are much higher than GEO and constitute the major radiation source. Contributions by lower-energy solar protons and ions also go up.
- GCR dose rates are much higher than GEO (both SPE and GCR numbers show the loss of shielding from the outer magnetosphere)
- Overall cruise phase has somewhat less radiation than GEO, but the particle energies are higher. This has ramifications on semiconductor performance and the effect is non-linear.

Lunar Mission Radiation Environment

The Moon has no atmosphere nor magnetosphere. At this distance from Earth, only the long tail of the magnetosphere provides any protection. Therefore, the Lunar mission environment is the same as the Cruise Phase radiation environment with one notable exception.
ALL planets and moons provide shielding by their mass. The shielding is 100% for bodies of any appreciable size. For a spacecraft orbiting the moon, there are two effects that result in a significant reduction of actual radiation levels. The first is Lunar body shielding of the spacecraft from the Sun emitting the SPE component of radiation dose. Here a simple orbital simulation that includes the occlusion of the Sun's particle emissions by the Moon as a function of orbital position will produce the desired moon body attenuation. The trick is to properly constraint the simulation by specifying the spacecraft to sun line-of-sight access intervals and integrating all the vector contributions for each line-of-sight path. Intuitively, if the spacecraft is in orbit close to the Moon, the occlusion of Sun by the Moon will be 100% for about half the orbit. A higher lunar orbit will result in lesser occlusion resulting in a higher dose from the SPE component.
By contrast, GCRs are also blocked by the Moon, but now the occlusion calculation has to be done in spherical coordinates as a percentage of occlusion over the 4Pi Stearadian sphere representing the isotropic GCR dose. Occlusion percentages are then applied to the GCR component of the dose. Calculating the occlusion percentage and the resulting reduction in dose has to be done for all spherical angles by integrating all the line-of-sight vectors from open space to the spacecraft.

For the lunar surface, local topography can produce even more shielding. In conclusion, lunar mission radiation levels are the same as open space at the Moon distance minus the effect of body and terrain occlusion.

Mars Mission Radiation Environment

A presentation to the NASA Advisory Committee (NAC) regarding the results of the most recent Mars radiation dosimeter experiment aboard Curiosity is used as the basis for this analysis.[vii] Although SPENVIS has Mars radiation models, the NAC briefing contains updated measurements. The Cruise Phase section is relevant until the spacecraft is close to Mars. Then one uses the local Mars measurement data, obtained in both the cruise phase and on the surface using the MSL-RAD dosimeter instrument aboard Curiosity.. These dosimeter measurements constitute the best radiation data to date from Mars as analyzed and presented in 2017.

The Curiosity Mars Science Lab (MSL) measured radiation during its cruise phase. The NAC briefing cites the SPE and GCR cruise-phase doses to be approximately three times the dose on ISS. The numbers show a dose rate of 40 Rad/day from solar particles, with SPE events producing an aggregate increase over mission duration of about 5%. The graph below shows the cruise-phase radiation measurements, including three SPE events. The GCR component produces the baseline radiation dose cited at 45 rads/day. The dose rate during SPEs can be 10 to 100 times that of average, which increases radiation tolerance requirements. However, given the short duration of SPEs, the contribution to overall TID is about 5%.

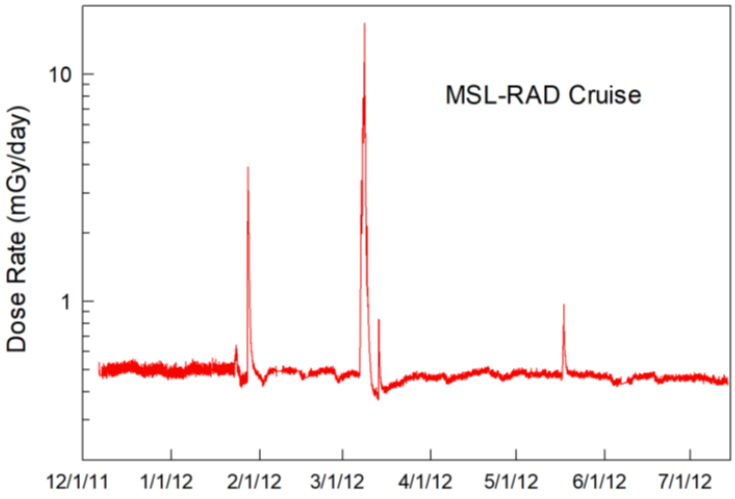

Figure 5 Mars Cruise Phase MSL-RAD Measured Radiation Levels

The MSL-RAD instrument also measured radiation levels on the Martian surface after landing showing a factor of 2.5 reduction on the surface vs cruise phase. The planetary body will shield spacecraft in orbit or on the surface of Mars and the treatment is the same as that for the moon – calculate the degree of occlusion by the planetary body and terrain as a function of position and reduce the dose proportionately. In addition, the thin Martian atmosphere also blocks solar particles and GCRs, reducing dose at the surface. The briefing cites Mars surface radiation levels at the orbital dose divided by a factor of 2.5. Using the dose numbers above, this puts the surface dose rate at 34 rads/day. The graph below shows the surface radiation levels measured by the MSL-RAD instrument at about 22 to 30 rads/day. (1mGy=100 Rads)

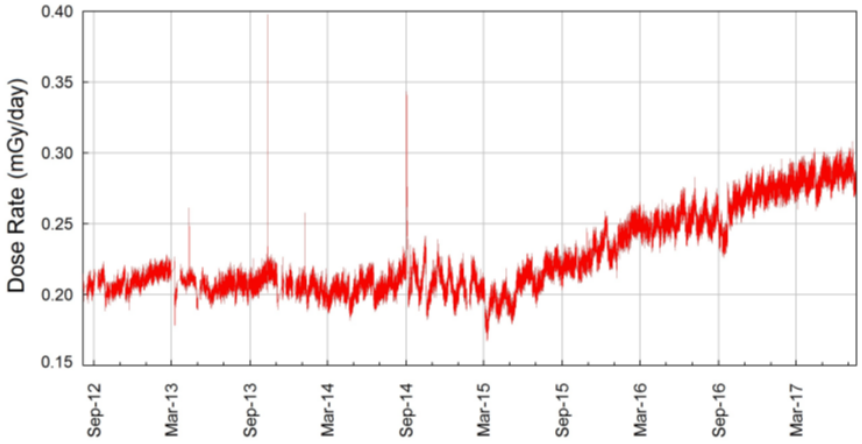

Figure 6 Mars Surface MSL-RAD Measured Radiation Levels

The briefing compares Mars dose rates to that on the ISS, so this correlation is used to verify the numbers produced by SPENVIS for LEO-ISS. The only consideration is the thickness of the shielding used for determining TID over a year. Since the MSL-RAD instrument is designed to measure radiation levels, it probably uses a minimum amount of shielding. On the surface, there is no material between the instrument and the environment and the instrument drawings show no shield over the detectors. SO – a shielding thickness of only 1 mm aluminum is assumed. The table below shows the direct comparisons, which are favorable.

Table 1. ISS vs Mars Cruise and Mars Surface Annual TID Comparison

Annual Mission Radiation Dose (Rads Si) with 1mm AL Shielding

Mission	Solar Protons	RAD	RAD	Total Dose
	Total Protons	Rad/Day	Tot/Yr	Rads (Si)
LEO ISS SPENVIS	6735			6735
ISS-RAD		24	8760	8760
CRUISE SPENVIS	18125			18125
MSL-RAD Mars Cruise		45	16425	16470
MSL-RAD Mars Surface		22	8030	8052

As an additional crosscheck, the ISS has a similar dosimeter aboard, called ISS-RAD and the following graph compares the results from the two instruments, verifying that the ISS dose is similar to the Mars surface dose and that the cruise phase dose is about 2.5 times that of the ISS dose. Note that while TID numbers are similar, GCRs dominate the Mars radiation. The numbers for LEO-ISS and CRUISE DRMs from the SPENVIS simulation are also shown for comparison. The number are comparable across the board.

Orbital Radiation Analysis

The magnetosphere traps the protons and electrons from the solar wind and greatly amplifies their ENERGY and concentrates the flux as well. The magnetosphere creates a giant cyclotron and increases the trapped particle energy by orders of magnitude. Now trapped particles become relevant to SEUs, and now both the trapped protons and the electrons can contribute to

upsets. These trapped radiation particles are localized into belts around the Earth, terminating at the magnetic poles.

In open space beyond the effects of the magnetosphere, we now get much higher solar flare energies and much higher GCR rates due to lack of the magnetospheres' shielding. Note that there are no trapped particle effects because there are no trapped particles for GEO and higher orbits. Solar flares occur for a period of hours at an average rate of about four per year, although this can change significantly depending upon the Sun's activity. Solar flares emit protons and electrons at much higher energies than the solar wind > 10 MeV and include He nuclei as well. During solar flares, significant upset occurs in avionics and flares also contribute significantly to total dose.

Solar flares are not the only phenomenon due to the Sun's internal activity. Solar protons and ions that have higher energy than typical for the solar wind are being ejected virtually all the time. There is an inverse relationship between the intensity of the solar flare and the interval between them. The graph below shows the curve used by ESP for modeling SPEs, and events ejecting in excess of 10^6 particles over the entire flare event occur ten times a year. By contrast, events of greater than 10^9 total particle fluence occur once every 10 years. These statistical models are built into the radiation simulation tools and have a good correlation with measured events. Solar protons and ions become far more important beyond GEO due to loss of the magnetosphere's shielding.

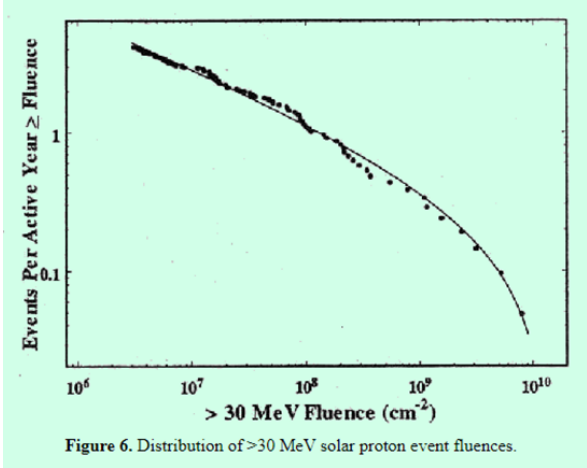

Figure 6. Distribution of >30 MeV solar proton event fluences.

Figure 7 ESP Model Correlation with Measured SPE Events and Energy

GCRs are isotropic high energy Alpha particles which are He nuclei. They contribute significantly to avionics upset rates and this is particularly true when there are no shielding effects from atmosphere or magnetosphere. Therefore, the two regimes (LEO and GEO+) are very different, hence, the focus on determining upset rates from the solar flare and GCR simulations beyond LEO. Separate orbital cases require different analysis for radiation effects because the dominant radiation phenomena are different. LEO – trapped particles dominate. In GEO, flares and GCRs dominate. GTO is a hybrid – trapped dominate for 2 hours of the 24 hour day, GEO environment otherwise. During the two dips/day, we get the full impact of the Van Allen belts when traversing these altitudes.

Modeling Comparison to NASA References

It is useful to compare how our trade study simulations compare to the ones performed by other NASA engineers. Of particular utility is the briefing done by JSC engineers[6]. The TID graph below uses much the same assumptions as our DRMs, so is an effective crosscheck.

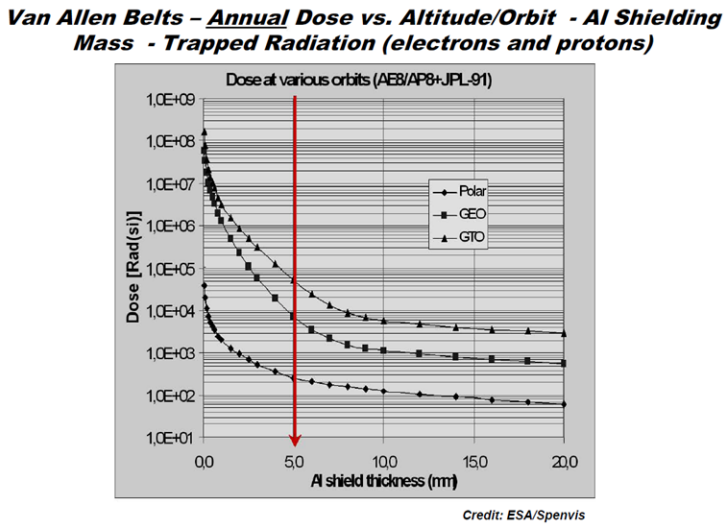

Figure 8 TID Graph from Koontz:

The table below shows the TID values from the TID graph above as compared to the value obtained from the DRM simulations. All values assume 5 mm AL shielding. The SPENVIS simulation numbers contain SPE and GCR numbers obtained from the SLS Reference.

Table 2 Comparison of NASA JSC DRM TID to SPENVIS TID Values

DRM Case	Koontz Ref (Rads)	SPENVIS (Rads)
GTO	50K Rad	60 K Rad
GEO	8K	6K
Polar	250	333

TID values used as requirements for avionics have a wide range, mostly due to different shielding assumptions. More than a 10:1 range of TID values occurs between 2mm and 5mm of AL shielding, for example. Therefore, the TID values from the reference and the simulations are considered comparable in that both use 5 mm AL for the shielding thickness. As can be seen, the TID values obtained by our SPENVIS simulations compare favorably with those used by other NASA avionics engineers.

SEE Rates are far more difficult to compare given their first-order non-linear dependency upon semiconductor device LET values. Small differences in LET can have a major impact on SEE rate depending upon the radiation environment spectrum and flux. The best comparison is presented to the left, where the accuracy of the various SEE models is compared against flight data. This trade study uses the CREME96 SEE method, which is shown to have a good correlation with space flight data over several orders of magnitude.

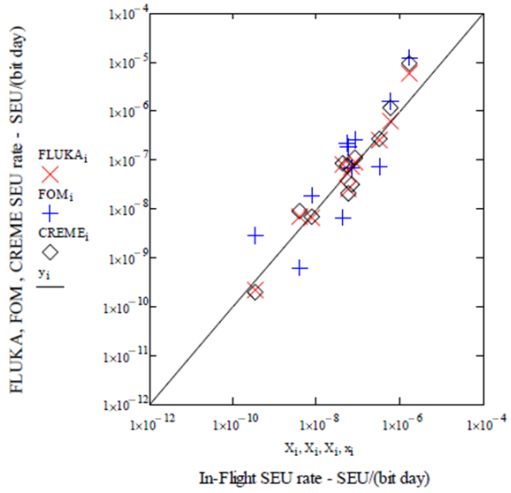

Figure 9 Predicted SEE Rate Correlation to Flight Data from Koontz

As a verification of SEE prediction the following map of MDM memory upsets vs orbital position of ISS looks just like the picture of radiation dose in LEO. These are detected and corrected errors in the memory. This is exactly what it should be if the models and predictions were correct and are truly random. A derived conclusion is that memory errors within the MDMs are entirely caused by random SEUs, which reflects a mature design that conforms to avionic system requirements. Note the lack of upsets in the benign regions.

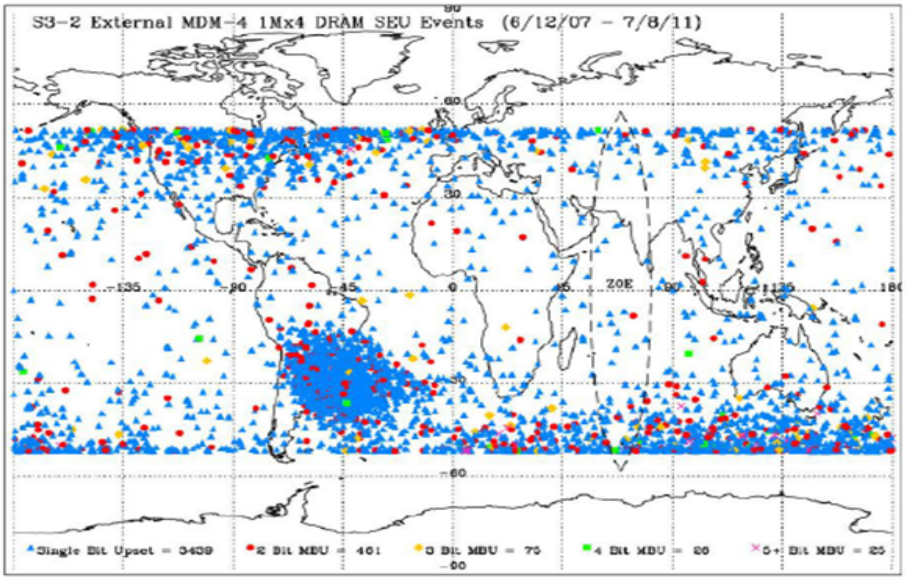

Credit: NASA

Figure 10 Map of MDM Memory Upsets aboard ISS

Design Reference Mission Total Integrated Dose

The SPENVIS simulation environment directly provides Total Integrated Dose (TID) numbers for the entire mission duration, which has been set to one year for each DRM.[viii] As the radiation sources and intensity vary significantly with orbit, there are significant variations in TID. The SHIELDOSE-2 code run within SPENVIS is used to integrate the contributions from trapped protons and electrons and solar protons/ions and GCRs and produces a report and graph of TID versus aluminum shielding thickness. Please note that shielding is required for avionics used in space to absorb the low energy protons and electrons which contribute to TID and device failure, but which can easily be stopped by even a minimal shield. The graph below demonstrates the exponential effect of shielding to reduce TID. At 2mm AL, the electron contribution becomes negligible, and at 5 mm the proton shielding effectiveness bottoms out. Subsequent thickness of shielding is not as effective as the first 5 mm of AL have hardened the beam to allow easier penetration of additional aluminum. This beam hardening effect limits the effectiveness of shielding, so multiple materials are often used to compensate. For example, a tantalum foil can be added to the chip package and the additional shielding can be calculated using SPENVIS features. Differences in TID tolerance can often be traced to different shielding assumptions and the effect is exponential as the graph shows.

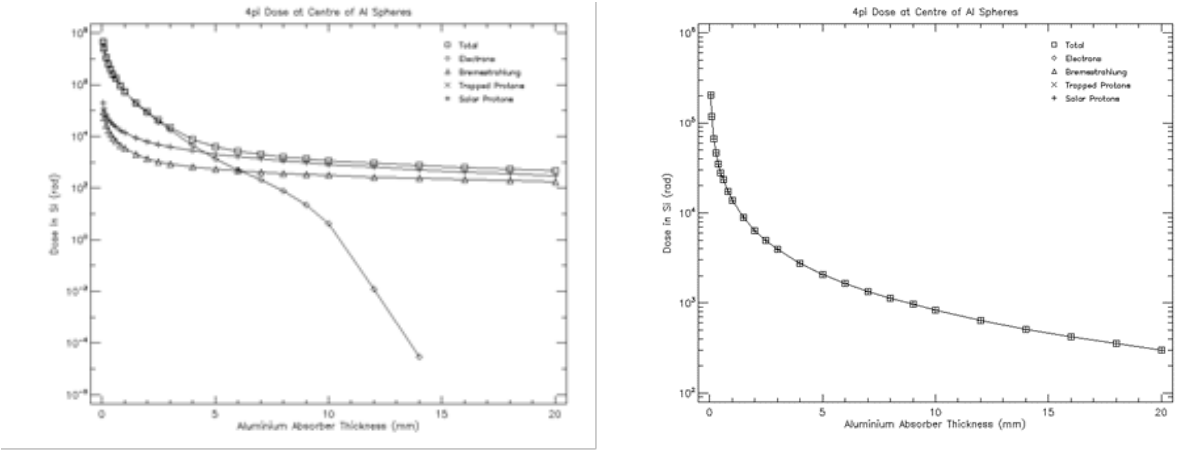

Figure 11 TID Graphs for GEO and Lunar DRMs

The two graphs dramatically show the difference between TID for GEO vs the Lunar DRMs due to the different radiation environments. The GEO has contributions from trapped particles and solar protons, but the Cruise phase (Lunar) only has contributions from the solar protons, which have higher energy spread than the trapped protons. Note that beyond 5 mm of AL, one can only obtain an additional factor of two reduction in TID by using 20 mm of AL. That is, shielding effectiveness drops significantly after beam hardening occurs.

The SHIELDOSE 2 includes the contributions from trapped electrons/protons, Bremsstrahlung and solar protons, but does not include the contributions from energetic solar flares and GCRs. The method for including these effects varies, but the one used for this trade study is based on the Radiation Requirements Doc for SLS.[ix]This document simply adds 30 rad for each solar flare event, which occur four times a year on average. This results in an additional TID of 120 Rads per annum. The SLS document also specifies a similar method for GCR contributions, adding just 10 Rad a year from this source. The TID radiation table below summarizes the analysis for each DRM.

Table 3 Calculated DRM TIDs with 5 mm AL shielding

DRM	Total Trapped	Total Solar Protons	Total SPE	Total GCR	Total TID
LEO Zero	11		120	5	136
LEO ISS	305		120	5	430
LEO POLAR	208		120	5	333
GEO	5800		120	10	5930
GTO	153000		120	10	59630
Lunar cruise	0	2000	120	30	2150

LEO-Zero is our benign environment case and accumulates nominal TID. Oddly enough the 51 degree ISS inclination produces slightly higher TID than polar orbit, because the spacecraft spends a bit more time in the South Atlantic Anomaly. ISS is considered a moderate LEO environment. Note how LEO is dominated by trapped protons, but that solar flares contribute a significant dose, even though they are short duty cycle events at infrequent intervals. The contribution to TID from GCRs increases once beyond the magnetosphere.

Design Reference Mission Particle Flux

While TID dominates by limiting the mission duration for avionics due to accumulated damage in semiconductor materials and devices, particle flux (instantaneous rate) or fluence (average rate over time) directly cause SEEs, which result in computational and memory errors. These errors compromise the function of avionics and have to be kept below the level at which they affect mission operations. Setting the desired SEE rate requirements for missions is highly dependent upon the function performed by the avionics and the conditions under which it operates. For this study, only a comparison of particle flux is conducted to understand what environments pose the greatest challenge. It is the interaction of the particle species and energy with silicon and the circuits that produce SEEs. So, while SEE rate is dependent upon the flux, the actual rate can only be predicted using the embedded numerical simulation tool CREME96 or equivalent. This is because the upset susceptibility of avionics is directly related to the LET of the semiconductors used.

SPENVIS produces graphs of particle flux vs energy and particle flux vs orbital time. The first one determines the basic upset rate and the second identifies the regions where maximum upsets are expected to occur. Only certain energy ranges (~1MeV to 100 MeV) are likely to cause upsets, even though the incident radiation spans a much larger range. Flux is expressed in particles per square centimeter per second. Each particle has only a small probability of creating an upset, dependent upon device parameters (LET), so flux is much higher than upset rate. An effective cross-section of 10E-5 is typical, which results in one SEU per second with a particle flux of 10E5/sec-cm2. For the table below, the flux at 50 MeV is considered the midpoint for relevant energy levels so was chosen to represent the average flux derived from the Flux vs Energy graph. The maximum flux is the peak value obtained from the flux vs orbital time graph. The resulting table is shown below

Table 4 Design Reference Mission Flux and Fluence

Mission	Trapped Solar Particles				Solar Protons	Solar Flares		GCR
	Proton		Electron		Protons	Proton	He Ion	Proton, He
	Flux@50 Mev /cm2-sec	Max Flux >0.1 MeV	Flux@50 MeV /cm2-sec	Max Flux >0.1 MeV	Fluence@50 MeV /cm2	Flux@50 MeV /m2-sec-sr	Flux@50 MeV /m2-sec-sr	Flux < 100 Mev /m2-sec-sr
LEO Zero	3	200	1	400	550	0	0	92
LEO ISS	45	20000	1000	4000000	550	1000	25	500
LEO Polar	30	10000	10000	10000000	550	3000000	20000	500
GEO	0	0	0	0	20000000000	3000000	10000	3100
GTO	1000	100000000	0	0	0	1000000	1000	2800
CRUISE	2000	0	0	0	30000000000	100000000	1000000000	3200

Effects on Semiconductors

There are two effects resulting from radiation exposure in semiconductors.[x] The first is damage due to accumulated radiation dose that alters the characteristics of the transistors resulting in functional failure over time. The radiation dose can also cause damage in the Silicon crystal lattice, which can also cause functional failures. Failures due to TID cannot be reversed and it is the accumulation of radiation damage over time that is of concern. Therefore, TID is both a characteristic of a given radiation environment but is also used as a requirement for avionic

systems. One can take the estimated mission TID value, add a safety margin and use that for the TID requirement levied against the avionics.

The second radiation fault modes are Single Event Effects (SEE) caused by a single particle depositing energy in the Silicon resulting in production of electron-hole pairs.[xi] These charges then cause changes in memory state and other effects that can result in functional interrupts. SEE can be bit flips (Single Event Upset (SEU)), functional failures (Single Event Functional Interrupts (SEFI)), or latchup (Single-Event Latchup (SEL)). Please note that unlike TID, which is the integration of radiation energy and flux over time, SEE is driven by the instantaneous impingement of particle energy into the active circuits of the avionics. Therefore, the species (electrons, protons, ions), their energy and their flux are all relevant in causing memory or state changes or even functional failure of avionics.

High-level requirements for space avionics derived from functional reliability can be summarized:

- Avionics shall meet the TID requirements for dose rate over entire mission duration
  - Integrate dose over mission profile and duration to determine TID
  - Add shielding to reduce TID requirements
  - Select semiconductors with TID rating sufficient to meet mission requirements plus margin
- Avionics shall meet computational reliability requirements for the mission function performed
  - For human space flight-critical functions, double fault tolerance is required.
  - The same requirement is levied for aircraft
  - For life-critical functions, double fault tolerance is also required.
  - For mission-critical functions, single fault tolerance is usually required.
  - For non-critical functions, fault tolerance may not be required.
  - Fault tolerance also includes time response and latency bounds
  -

Unfortunately, certain SEE failures are permanent. For latchup, a circuit is put into an anomalous state by particle and charge injection. For example, both transistors in a flip flop can turn-on and stay-on, an anomalous state that results in high current through the flip flop. A transient SEL can be cleared by a power cycle, but a permanent SEL generally results in device failure. The first step in hardening avionics for radiation is the elimination of ALL permanent SEL faults within the chip for the radiation levels encountered in the mission. Mitigations are often done at the chip fabrication level by using Silicon on Insulator (SOI) fabrication and similar methods, which provide better isolation of circuits.

Once a semiconductor does not fail under the anticipated radiation dose rate, it can be protected against changes of memory or state, which result in program execution failures or data errors. Mitigations in this area are the use of error detection and correction (EDAC) circuits at various points in the avionics system. To determine system-level SEU rate, the device error rate is multiplied by the number of bits in the system and then reduced by the effectiveness of the EDAC circuits.

There are established methods for calculating the rate of SEE upset in semiconductors, based on atomic physics. The charge deposition from a radiation particle in a Silicon circuit is given by the interaction cross section of that particle with Silicon. The Linear Energy Threshold (LET) is the energy required to deposit an electron-hole pair into the active layer of a semiconductor. The LET is the distance a given energy particle travels in the Silicon before it is stopped. Low energy particles deposit their energy in the surface layer and are blocked by the avionics shielding. High energy particles just shoot through the semiconductor without depositing any energy in the semiconductor. Therefore only a certain range of particle energies (which differ by species) can create charge effects in semiconductors leading directly to SEEs.

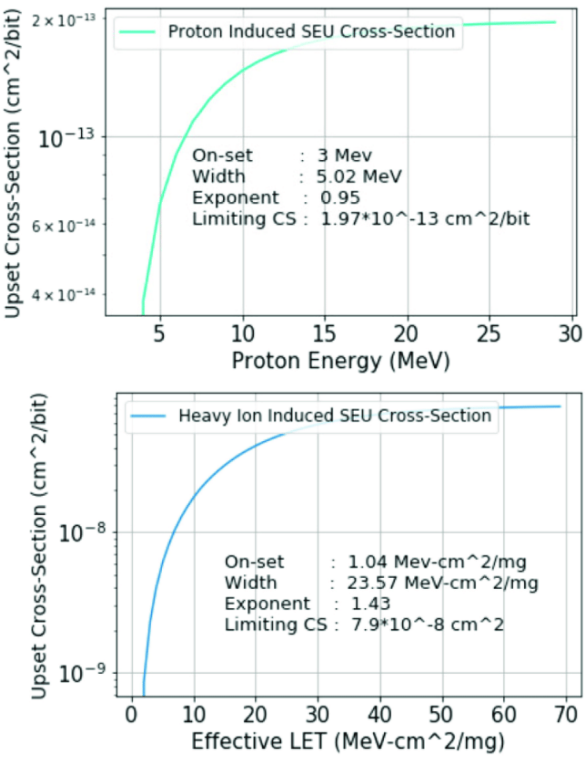

Figure 12 Semiconductor LET Graph for Protons and Heavy Ions [xii]

This range is primarily 1 MeV to 100 MeV for protons. A typical LET curve for protons and heavy ions for a typical memory device is shown below, which plots the interaction cross-section probability vs the particle energy.

The math required to calculate the rate of SEE for a given semiconductor consists of integrating the energy/flux spectrum of the incident radiation by the device LET values to generate a device-level rate of upset. That is, one needs two curves: the graph of incident energy vs flux from radiation modeling and the graph of the LET cross-section vs particle energy to determine the rates at which particles are likely to cause an upset. LET values for semiconductors are determined by radiation testing:

- One uses protons or ions on the test chip from an accelerator producing a known energy vs flux source. Note that an accelerator produces flux levels many orders of magnitude higher than encountered during space missions.
- The test chip is de-lidded. That is, there is no material between the particle beam and the semiconductor. Any material causes shielding effects that are difficult to analyze.
- The test chip is running a test program that is able to detect and count SEEs. The count of SEEs over time at a specific energy level is indicative of the LET at that energy.
- The radiation test results allow producing a LET graph by curve fitting a Weibull function to the test data points.
- This LET graph is the primary product of radiation testing and is a characteristic of the devices produced on a given fabrication line.
- This same LET graph can be used with natural radiation sources derived from the SPENVIS modeling tool to predict SEE rates within the target mission environment using the CREME96 codes. These predicted SEE rates are then used to see whether the avionics meets the SEE rate requirement for the actual mission.

That is, radiation testing in an accelerator is absolutely required to characterize the avionics devices used on the chip. The LET values vary considerable by size of device, its construction and substrate. Please note that an accelerator produces much higher flux than the natural sources and that the energy values are also highly dissimilar. Radiation test conditions are orders of magnitude higher than mission environments, yet the method of integrating incident energy with LET works well even over such a range. The LET values required for space missions are actually well established and very few commercial devices meet them. Hence the need for radiation engineering at the fab and device level. LET values apply to the active devices within the semiconductor chip.

Please note that the mathematical treatment is not precise – only a few energy/SEE rate points are obtained during radiation testing and then the proper curve is fit to that data, filling in

the rest of the device properties. Also, the effect of shielding by other materials is complex and ignores the production of secondary particles. Finally, only certain energy points are used for determining the SEE rate, not a full-up integration. These methods yield estimates that can be used for setting requirements for devices and testing. Further validation under actual mission conditions is needed for critical applications.

The flux of solar protons and ions plus the contributions from GCRs can be used to estimate the raw upset rate of semiconductor memories. This raw rate does not include the effect of any shielding, so tends to be an overestimate. The two graphs below show the proton and ion flux for the lunar DRM to provide the relevant radiation environment numbers. Note how solar protons range from 10^9 to 10^{11} protons/cm2-sec and solar ions are much lower at 0.1 to 300 ions/cm2-sec on average (fluence is averaged over 1 year). The total upset rate is the sum of these two contributors in first order and is expressed as the number of upsets per second per memory bit.

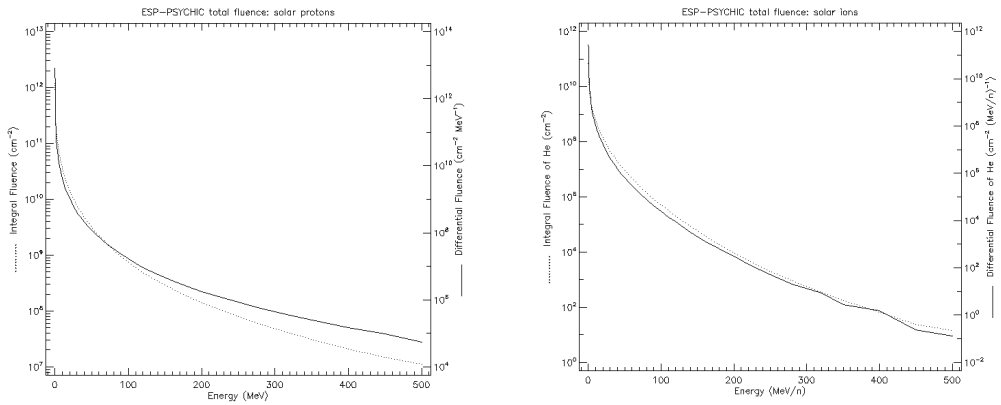

Figure 13 Lunar Transit Solar Proton and Ion Flux

To determine system-level SEE radiation tolerance, one must multiply the device upset rate by the number of active bits in the system. For large memory arrays, this can be a huge multiplier ($16X10^6$) for a 2 MB memory array typical for modern CPU caches. Therefore raw SEE rates have to be low enough to allow creation of large digital systems, which means using radiation-qualified memory chips. However, certain mitigations, such as Error Detection and Correction circuits added to memory can greatly reduce the effective upset rate (typically by 10^5) by correcting the vast majority of data bit flips before they cause computational errors.

The Table below contains the results of upset rate calculations done for two different devices, whose LET curves were presented earlier. Very high rates of upset are seen with both devices – and inspection of the numbers shows the reason: While the interaction cross-sections are rather low, the proton flux in lunar transit is very high, resulting in a high rate of upset. Accounting for the protective effect of ECC, the rates come down to less than one upset per second. The actual rate is the summation of all the upset rates, but certain energies predominate. Note that these are the rates for unshielded electronics. The effect of shielding material is highly complex, cutting out the lower energy particles significantly, which tend to cause a greater rate of upset due to higher flux. In practical terms, shielding can lower the SEU rate by a factor of 10 to 20 over unshielded avionics. Taking this into account, one finds that we now see an upset every 10 seconds or more, ample time to allow memory scrubbing to eliminate accumulation of errors. Please note that higher energy particles cause secondary particles within the shielding material and that these secondary particles can then cause even greater upset rates. Therefore, a full program of ground-based radiation testing followed by flight verification is needed for critical avionics systems.

Table 5 Calculated SEU Rates for Example Memory Chips

Device	LET	Cross-section	Flux	SEU Error Rate	Memory Array	Memory Array	Notes
	MeV-cm2/mg	cm2/bit	part/cm2-sec	SEU/bit-sec	Error Rate in SEU/sec	Upset with ECC	Assume
Low-tolerance example							10E5 reduction with ECC
Proton	3	4.00E-14	1.00E+12	4.00E-02	6.40E+05	6.40E+00	2 MB RAM
	5	6.00E-14	1.00E+11	6.00E-03	9.60E+04	9.60E-01	
	10	1.00E-13	2.00E+10	2.00E-03	3.20E+04	3.20E-01	
	30	2.00E-13	1.00E+09	2.00E-04	3.20E+03	3.20E-02	
Heavy Ion	1	1.00E-09	3174.603175	3.17E-06	5.08E+01	5.08E-04	
	10	2.00E-08	3.17E+02	6.35E-06	1.02E+02	1.02E-03	2 MB RAM
	50	8.00E-08	3.17E-02	2.54E-09	4.06E-02	4.06E-07	
M168X 65 nm SRAM							
Protons	15	1.00E-14	1.00E+10	1.00E-04	1.60E+03	1.60E-02	2 MB SRAM
	50	1.00E-13	2.00E+09	2.00E-04	3.20E+03	3.20E-02	
	100	1.00E-11	1.00E+09	1.00E-02	1.60E+05	1.60E+00	
Heavy Ions	15	2.00E-07	3.17E+00	6.35E-07	1.02E+01	1.02E-04	
	50	1.00E-04	3.17E-02	3.17E-06	5.08E+01	5.08E-04	
	100	3.00E-04	3.17E-03	9.52E-07	1.52E+01	1.52E-04	

Experimental Mission Profiles

The RadNeuro team at NASA ARC is conducting early space missions for evaluation of commercial and hardened NMC processors. It has identified multiple flight opportunities, and has delivered an experimental payload for the first mission, TechEdSat 13 (TES13) currently in LEO, and is developing a series of payloads for additional missions. The proposed missions range from LEO to polar to GTO spanning several years. The radiation environment for two experimental space missions was characterized over the nominal mission duration and was used for defining the payload requirements presented below. These missions provide examples for applying the radiation modeling and hardening techniques presented in this paper.

TechEdSat13 Mission and Payload

TES13 is a 3U CubeSat that is based on a spacecraft design matured by various student interns over many years. It is fully custom and can host various payloads and technology demonstrations. TES13 was launched aboard the Virgin Galactic Cosmic Girl aircraft from Long Beach airport on Jan 13, 2022 to 500 Km altitude at 45 degree inclination, which is a benign LEO orbit. The objective was to determine whether transitions through the South Atlantic Anomaly (SAA) would cause computational errors in commercial NMC hardware. The experiment is on-going.

This LEO orbit encounters significant radiation only when traversing the SAA. Certain orbital parameters are relevant:

- 500 KM orbit has a period of 1:34:37 so get 15.89 orbits/day
- South Atlantic Anomaly covers about 105 deg, see Figure Below.
- Should get SAA crossings for 4 consecutive orbits. Maximum duration crossing is estimated at 11.4 minutes, but the bulge is not uniform, so some orbits will spend less time in the SAA.

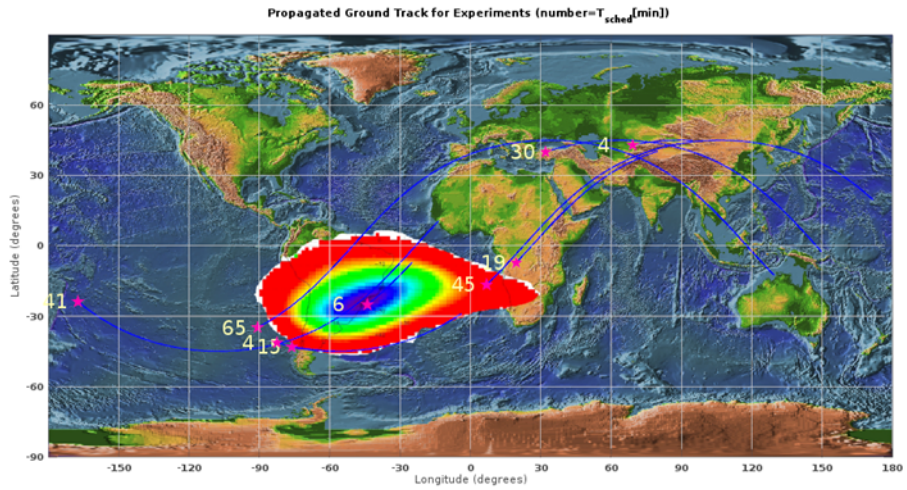

Figure 14 TES13 Ground Track within the South Atlantic Anomaly

Certain key graphs help explain the radiation environment encountered. Recall that at this low altitude, only the trapped radiation fields impact the avionics. The graph below shows the proton radiation flux vs orbital time. Flux of up to 10^4 particles are seen during traverses of the SAA, but only for short intervals of a minute or so. Virtually no other radiation is seen during other parts of this orbit. The energy and the number of particles are sufficient to cause upsets in commercial avionics. Other contributions are negligible. The second graph below shows the low TID accumulated during a full year on orbit. The TID value of 6K Rad is so low that virtually any commercial semiconductor will not suffer hard failure.

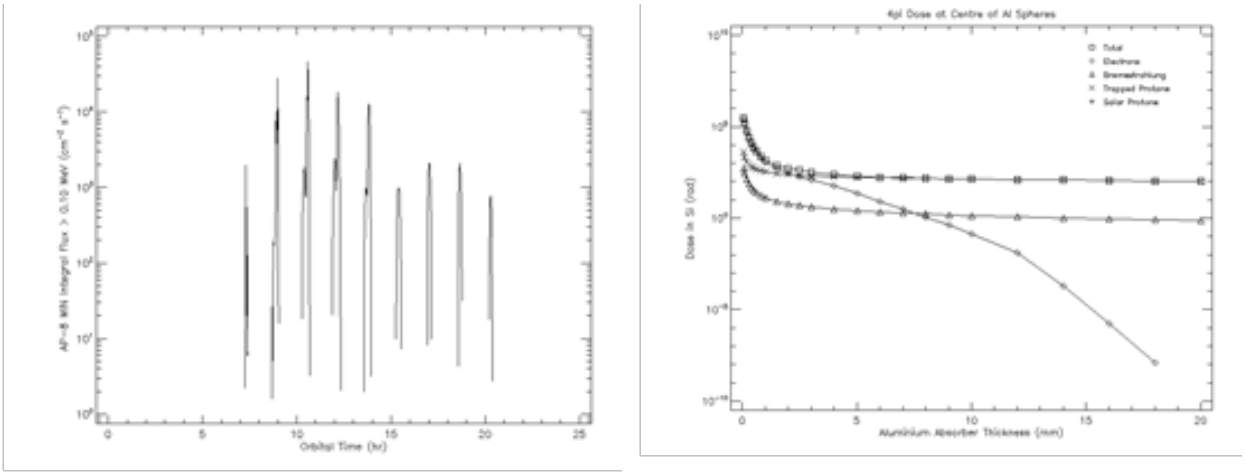

Figure 15 TES13 Proton Flux vs Orbital Time and TID per annum vs Shielding

GTO Mission and Payload

Another small spacecraft mission will fly a small spacecraft in a GTO to measure radiation levels. As this flight provides a wide range of significant space radiation, it can be used to determine the response of prototype NMC processors to these natural radiation sources. From the experimental data, it should be possible to determine basic SEE rates for the hardware. These rates can be measured without NMC-specific radiation fault mitigation and then with the mitigation enabled, getting early data on radiation-tolerance of the multiple NMC processors being flown aboard the spacecraft. The spacecraft itself is hardened against radiation effects, and the experimental NMC hardware will be designed to provide reliable data even in the higher radiation environment. The graph below is the GTO orbit and shows two and a half transitions from GEO to LEO per day. The SPENVIS simulations for GTO describe this mission very well and the requirements for the NMC Payload are derived directly from them as an example. Graphs of the orbit, proton flux species and proton flux vs orbital time are shown below. They

emphasize the transition through the Van-Allen belts where maximum proton dose occurs. The table below help describe how the radiation environment for the mission is mapped to the avionics requirements.

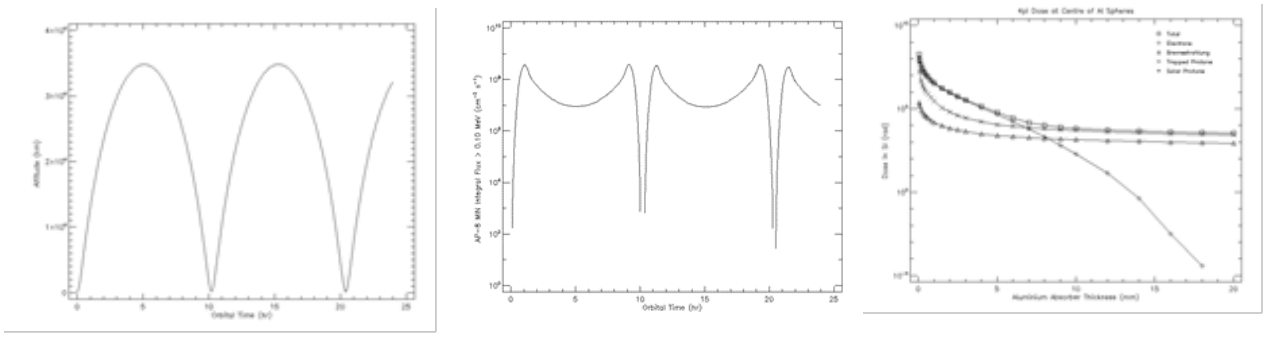

Figure 16 GTO Orbit, Proton flux vs Orbital Time and Annual TID

The first graph shows the peak trapped proton flux in excess of 10^8 protons/cm2-sec during the dips through the trapped belts. A value of 10^7 is obtained at the apogee comparable to GEO. These flux values are used as inputs for SEE rate predictions using the method presented in a subsequent section of this trade study. The mission TID requirements can be derived directly from the SHIELDOSE-2 graph and is expressed as rads/year, and the total approaches 100K rads, which generally requires radiation hardened avionics. Therefore, the host computer and other functions that must operate reliably should be good to 100K Rads and that is the requirement value cited below.

- GTO TID Requirement: 100 K Rads
- GTO SEE Requirement: Operate reliable up to 10^7 protons/sec-cm2

However, most COTS semiconductors do not meet that TID requirement, so that some experimental hardware has to be derated in terms of mission duration. For example, an NMC processor that has 30K rad TID tolerance would only be expected to operate for 0.3 years, or 4 months before failure. The payload design will use the full 5mm of aluminum shielding and will consider the use of Tantalum foil for the CPU chip and other sensitive components. As this is an experimental payload, different elements will have different TID ratings. For avionics used in flight critical applications, every part must meet or exceed the expected mission TID levels. For the GTO payload, cost and schedule constraints prevent using a radiation hardened host processor, so a radiation tolerant processor product can be used where the CPU SoC has known radiation characteristics and the rest of the processor board is outfitted with selected memory incorporating ECC. Other functions are implemented in Triple-Modular-Redundancy (TMR), greatly reducing SEE rates. The TID rating of 30K Rads ensures that it will run for at least a third of a year in GTO. Unfortunately, the radiation tolerant CPU board being evaluated did not provide the needed SEE performance. The candidate board experienced significant upsets at proton rates of 10^6 particles/cm2-sec so did not meet the requirements of the GTO mission. This is due to the use of standard memory products, not the hardened ones needed for such a mission. The memories were still vulnerable despite ECC and other mitigation techniques and this was true of the processor chip cache memory as well.

Radiation Mitigation Techniques for Neuromorphic Computing

Since many neuromorphic computing chips are based on digital technology, hardening them against radiation effects follows the conventional methods applied to digital logic. The most important function to preserve in avionics is the memory, which suffers bit upsets that may not be detectable nor correctable. Unfortunately, all memory will suffer bit upsets, with only the rate

of upset able to be mitigated by increases in semiconductor energy tolerance as expressed by the LET curve. Therefore, only architectural mitigations coupled with hardened memory chips can provide reliable operation. Moreover, there are many different kinds of memory in modern avionics and they are all vulnerable.

We analyze the conventional Von-Neumann avionics system from the processor outward, starting with the processor cache memory, which is based on small geometry SRAM. Virtually no COTS processors protect these caches and these caches are needed for maintaining processor throughput. Turning them off is a very bad solution. Radiation tolerance consists of providing either parity for detection of upsets or for ECC for correcting upsets. Note that when an upset is detected, the entire cache must be flushed and reloaded, incurring a small processing delay.

The next memory would be the DRAM used for main CPU storage. DRAMs are very vulnerable to SEUs and hardening can only be done to 100K Rad. Therefore, extensive use of ECC is required to preserve main memory validity including the use of background scrubbing programs to ensure all memory is read at periodic intervals and subject to ECC action. As the memory array SEU rate is directly proportional to the number of active bits in the array, sizing main memory to the minimum needed is good practice.

Non-volatile memory (NVM) remains an area of concern. Typically, single-level-cell (SLC) flash memory using a NOR configuration is used for space computer boot memory. Generally two banks are present, one for booting and the other for modification or backup. Note how redundancy is required for this function. For large NVM arrays replacing disk drives, triplicated flash is often used, also protected by ECC. This is because the flash memory devices themselves fail on-orbit. Triplication allows single device failure while still functioning correctly.

Correctness of function could be defined as a Figure of Merit for computational systems. Note that if an SEU error can be detected and corrected before the error causes a functional failure, this SEU has been fully mitigated. For reliable and correct computation, all SEUs need to be mitigated in all computational memory. This is the basis of many of the remaining methods used for SEU mitigation, computational redundancy, program rollback and reconfiguration to cover permanent faults. For example, a two CPU Self-Checking Pair (SCP) can be used as computational building blocks: disagreement between the two triggers recovery and can cover CPU cache errors using COTS processors. Watchdog timers can be used at various levels to initiate recovery or reboot if not inhibited by software within timeout interval. Voting architectures: multiple computational strings with software running same calculations, with the results compared in external logic; disagreement means that string has a fault. Hot backup uses an independent computer running different software that follows the main computer and takes over upon fault detection.

An interesting observation falls out from looking at system-level interactions. The time to detect and correct an error has to be less than the time interval between SEU events. This places an upper bound on raw SEU rates for computational systems. If the circuits upset faster than they can be corrected, the mitigation fails.

The digital circuits themselves can be protected against upset resulting in data errors or functional failures. The use of a six-FET DICE cell for a flip-flop reduces upset by orders of magnitude. Similarly, implementing full triple redundancy with voting is often used for FPGA circuits used in Aerospace. This is simply done by checking the TMR box in the FPGA CAD tool. This option requires 4X the circuit resources, yet is still common practice to achieve reliability for aerospace. Approaches such as asynchronous logic have been mentioned as reducing errors in digital systems.

One of the best ways of ensuring correct computational subsystem behavior is to monitor the computational system using a rad-hard set of circuits generally implemented using an FPGA. This foundational layer manages power to each of the CPU subsystems and can monitor power to detect transient SELs. If one monitors a CPU board during radiation exposure,

the first symptoms are anomalous currents caused by particle-induced charge. These currents can be detected and the affected chip power-cycled. The power cycling can be done in milliseconds in certain cases, resulting in only a minor timing glitch. For most cases though, the power cycling requires a full reboot of the CPU. Therefore, reboot time of the CPU can be an important factor for system recovery.

NMC circuits are much the same as CPU circuits, and a conventional host is included in many NMC chips. These hosts and the digital circuits associated with the NMC processor can be protected using the conventional means described above. However, NMC circuits do have parallel properties that can be exploited in novel ways. A basic NMC neuron circuit is a multiply-accumulate (MAC) stage fed by multiple inputs and routed to multiple outputs. The input/output routing is often done using a local high-speed network. The MAC itself uses fixed weights that form the neural model. Changes to these weight values will change the computation results, so ensuring reliable weight values after radiation exposure is the first line of defense for NMC. One basic difference is that the weight memory may be distributed across the chip, an architecture known as compute in memory (CIM). A method used for reliability enhancement would be to read-out the weight memory at periodic intervals and compare them against a golden image stored in reliable NVM memory managed by the host. Another method would be to use the large number of parallel neurons to encode a neural model that balances out the contributions from each parallel path. The thousands of other correct paths will then swamp out an error in one path. The NMC array could be partitioned into multiple sections, each performing the same computation, and then the results voted upon. This could be extended into temporal redundancy, with the NMC performing the same computation twice and the results voted upon. It is clear that taking advantage of the parallelism in NMC architectures can improve their radiation performance, but there is a lack of quantitative data.

New types of NVM can be used for either conventional or NMC processors. Magnetic spin ram or STT-RAM has shown TID tolerance beyond 2 MRad. Memristors can store analog values using phase changes in materials. Since Flash NVM tends to be the weak point in avionics, substituting STT-RAM can extend the useful mission range. A similar type of technology, the ferro-electric RAM can be substituted for DDRAM for main memory in high-radiation environments.

Analog circuits are also affected by radiation. Unfortunately, work in this area lags far behind work on digital circuits. For example, some of the softest components on a COTS CPU board are the voltage regulators and current sensors used for managing power. They change voltage value or fail at low TID. Replacement of these soft components with harder components is the trick for improving radiation tolerance. Radiation changes the threshold value of FETs, resulting in bias and voltage shifts. Only if these threshold changes are balanced out using circuit techniques will the analog circuit work reliably in space. Proof of radiation tolerance is by test, as these circuits tend to be novel.

Lastly, the techniques applied to harden semiconductors have to be used to keep upset rates within acceptable bounds, which vary by mission type and trajectory. These methods are expensive to apply, in that they require redesign of the chip. However, certain types of fabrication provide real benefits, like the use of Silicon-on-Insulator (SOI) fabrication to eliminate permanent SEL. Many chip designs can be ported to SOI from more conventional fabrication lines. Using larger geometry fabrication helps reduce radiation effects, but one loses the complexity and speed of the chip's function, and this port is not easy. The use of vertical FETS have been used for the Xilinx Virtex-5 line of radiation tolerant FPGAs. FinFETs are similar and have better radiation performance when compared to planar geometries of the same dimensions. However, FinFETs are getting much smaller, and are therefore not a real improvement for radiation tolerance. Radiation test data using modern fabrication techniques is being generated now, so this is a dynamic area of technology development. Other techniques are similar – guard rings around circuits to prevent charge migration, enhanced conductivity

substrates to ground out the stray charge and design libraries with greater device spacing are all used for improving radiation tolerance and many can be applied to existing chip designs retroactively. Simply slowing circuits down helps reduce SEU rates by improving timing margins, mitigating some charge effects.

Conclusions

The methods and tools outlined in this trade study represent the conventional way for determining the radiation tolerance requirements and mitigations applied to avionic systems. This trade study focuses on determining the hardware requirements for NMC processors used in space, which span a large range from LEO to Mars. The two basic radiation requirements are that the avionics system has to run for the required mission duration in the mission radiation environment, which can be modeled very accurately using the embedded models in the SPENVIS workbench. The expected duration is the time for the avionics to reach its TID rating and this must exceed the required mission duration plus a safety margin. For SEE: the avionics must survive the highest peak flux encountered during the mission, and may even have to operate through the radiation event. This is particularly true of planetary missions, where intense radiation fields can be present. The cruise phase of a mission allows unshielded solar protons and ions to affect avionics, so that solar flares become a major issue that can cause transient loss of function. It is essential to eliminate all destructive SEFI and SEL failure modes in the semiconductor circuits, since these faults cause full loss of function without recovery options. Hardening avionics at the device and circuit level consists of modifying chip layout libraries and circuits to increase their resistance to radiation-induced charge by using insulating substrates and guard rings for fabrication, which directly results in increasing the LET values for that specific chip.

By contrast, SEE mitigation is done by applying mitigation measures such as memory error detection and correction, watchdog timers and other circuits. This level of mitigation is required for any avionics, because SEE rates cannot be zero. Finally, architectural level mitigation techniques like self-checking pairs and triplicated voting schemes (TMR) are also required. Hardening avionics systems is a combination of device and fabrication engineering to harden the chips together with the appropriate shielding and SEE mitigation measures at the circuit and system level are required to ensure function over the flight phases where the avionics must provide correct results. NMC processors are fabricated using conventional CMOS digital logic, so the general methods of hardening avionics must be applied first. NMC processors work very differently than VonNeumann CPUs, so different mitigation measures are possible, but the analysis and implementation follows the methods outlined in this trade study.

References

[i] NASA System Engineering Handbook; NPR 7120
[ii] SPENVIS Manual: https://www.spenvis.oma.be/
[iii] Barth, NASA GSFC
[iv] Barth, NASA GSFC
[v] SPENVIS Help: https://www.spenvis.oma.be/
[vi] Space Radiation Effects on Spacecraft Materials and Avionics Systems; NASA/JSC/ES4/Steve Koontz; NASA/MIT Workshop 06/26/12
[vii] “Mars Radiation Environment – what have we learned?”; Lisa C. Simonsen LaRC, JSC; Briefing to NAC HEO/SMD Joint Committee Meeting; 2017.

[viii] SPENVIS Tutorial: Radiation models in SPENVIS and their accuracy; D. Heynderickx; SPENVIS User Workshop, Brussels 2013.
[ix] CROSS-PROGRAM DESIGN SPECIFICATION FOR NATURAL ENVIRONMENTS (DSNE); NASA SLS-SPEC-159; DECEMBER 11, 2019
[x] Applying Computer Simulation Tools to Radiation Effects Problems; IEEE 1997 Space Radiation Effects Conference Short Course; Janet Barth; NASA GSFC.
[xi] Analysis of LEO Radiation Environment and its Effects on Spacecraft's Critical Electronic Devices; Luz Maria Martines S.; Embry-Riddle Aeronautical University - Daytona Beach.
[xii] Prediction of solar particle events with SRAM-based soft error rate monitor and supervised machine learning; Junchao Chen,Thomas Lange, Marko S. Andjelković, Aleksandar Simevski; October 2020 Microelectronics Reliability Volume 114.